Astron. Astrophys. 329, 792–798 (1998)

ASTRONOMY AND ASTROPHYSICS

# Density effects on the electronic contribution to hydrogen Lyman $\alpha$ Stark profiles

**O. Motapon**[1,2]

[1] DAMAP and URA 812 du CNRS, Observatoire de Paris, F-92195 Meudon Cedex, France
[2] Département de Physique, Faculté des Sciences, B.P. 24157, Université de Douala, Cameroon

Received 23 September 1996 / Accepted 17 June 1997

**Abstract.** The quantum unified theory of Stark broadening (Tran Minh et al. 1975, Feautrier et al. 1976) is used to study the density effects on the electronic contribution to the hydrogen Lyman $\alpha$ lineshape. The contribution of the first angular momenta to the total profile is obtained by an extrapolation method, and the results agree with other approaches. The comparison made with Vidal et al. (1973) shows a good agreement; and the electronic profile is found to be linear in density for $|\Delta\lambda|$ greater than 8Åfor densities below $10^{17}\mathrm{cm}^{-3}$, while the density dependence becomes more complex for $|\Delta\lambda|$ less than 8Å. The wing profiles are calculated at various temperatures scaling from 2500 to 40000K and a polynomial fit of these profiles is given.

**Key words:** lines: profiles – atomic processes

## 1. Introduction

About fifteen to twenty five years ago, a unified quantum theory of spectral line broadening has been developed (Van Regemorter 1969; Tran Minh and Van Regemorter 1972) and applied to the wings of the Lyman-$\alpha$ line of hydrogen atom (Tran Minh et al. 1975; Feautrier et al. 1976; Feautrier and Tran Minh 1977; Tran Minh et al. 1980). The validity of the results were checked by comparison with those of the semiclassical theories of Lisitsa and Sholin (1972), Voslamber (1972) and Caby-Eyraud et al. (1975); but also with the experimental results of Boldt and Cooper (1964) and Fussmann (1975). This formalism was shown to be particularly adapted for the description of line wings. It was then found that simple dipolar semiclassical calculations are valid not too far from the line core, but that quantum theory must be applied in the far wings. Since then, many theoretical works of importance have been carried out on Ly$\alpha$. One can mention the recent calculations of Stehlé (1994), who has tabulated the profiles of Lyman, Balmer and Paschen lines of hydrogen using a formalism based on the Model Microfield Method. These calculations provide an improvement in the line core, as compared to Vidal et al.(1973), because of the dynamical effects of ions and the simultaneous strong collisions that are taken into account. One can also mention the works of Günter and Könies(1994) and also Könies and Günter (1994) that deal with quantum mechanical electronic widths and shifts of spectral lines (over the full profile) and the electronic asymmetry of Ly$\alpha$, based on the Green's function technique.

Very few applications were made with the quantum unified theory mentioned above because of the numerical difficulties in the far wings. Calculations were carried out only for the plasma conditions of experiments, for comparison. The aim of the present work is to use this formalism to study the density effects on electronic broadening of Ly$\alpha$. The theory is briefly presented in Sect. 2, followed by the analysis of the density effects in Sect. 3. Sect. 4 deals with the extrapolation method used to describe the contribution of the first angular momenta. The results obtained by this method are close within a good precision to those provided by the semi-empirical method of Feautrier and Tran Minh (1977). In Sect. 5, a comment is made on asymmetry; the contribution of the short range potentials such as quadrupole and polarization potentials is discussed. Last before the conclusion, Sect. 6 is concerned with the comparison of our results with those of Vidal et al.(1973), hereafter referred to as VCS, and their polynomial fit for temperatures varying from 2500 to 40000K, and detunings $|\Delta\lambda|$ below 80Å.

## 2. Theory

In the one perturber approximation valid in the wings of a line, the quantum lineshape of Ly$\alpha$ at the point $\Delta\omega$ of the profile is (Tran Minh et al. 1975):

$$I(\Delta\omega) = N_e \frac{\langle L_f S_f \| d_1 \| L_i S_i \rangle}{(2S_i+1)(2L_i+1)} \sum \int\int\int d\varepsilon_{i'} \hbar\rho(\varepsilon_{i'}) \times f(\varepsilon_{i'}) \frac{(2\pi)^3}{4k_{i'}k_{f'}} \left(2S_i^T+1\right)\left(2L_f^T+1\right) \times \left| \int_0^\infty G^* \left(\Gamma_{f'} |\Gamma_f| r\right) G\left(\Gamma_{i'} |\Gamma_i| r\right) dr \right|^2 \quad (1)$$

*Send offprint requests to*: O. Motapon

where $N_e$ is the electronic density, $\rho(\varepsilon_{i'})$ is the energy density of the initial states, $\varepsilon_{i'}$ is the kinetic energy of the perturber in the initial channel, $k_{i'}$ is the wave number in the initial channel, and $k_f$ is that in the final channel $\Gamma_f$, $f(\varepsilon_{i'})$ is the Maxwellian distribution; $\langle L_f S_f \| d_1 \| L_i S_i \rangle$ is the reduced matrix element of the atomic dipole, $S_i$ and $L_i$ are the spin and the angular momentum of the atom in the initial channel; $S_i^T$ and $L_f^T$ are the total spin and the total angular momentum of the colliding system. The sum $\sum$ extends over $\Gamma_{i'} = n_i' L_{i'} l_{i'} L_i^T S_i^T$ - where $l_{i'}$ is the angular momentum of the incident electron - the corresponding coupled channels $\Gamma_i$ and the coupled final channels $\Gamma_{f'}$ and $\Gamma_f$; $\Delta\omega$ is connected to kinetic energies of the perturber in the initial and final states $i$ and $f$. The radial wave functions $G$ are solutions of the coupled differential equations.

The details of the formalism and the approximations used (dipolar approximation for the potential, exact resonance, no-quenching approximation, etc) were discussed in the previous papers as well as its classical limit (Tran Minh et al. 1980). The lineshape finally reads:

$$I(\Delta\omega) = \frac{\pi^2}{m^2}\frac{\hbar^2}{\Delta\omega^2} N_e \int_{\varepsilon_{\min}}^{\infty} \hbar\rho(\varepsilon_{i'})\, f(\varepsilon_{i'})\, d\varepsilon_{i'} \frac{(2\pi)^3}{k_{i'} k_{f'}} \times \sum_{L_i^T=0}^{L_D} \left(2L_i^T+1\right) \langle L_f S_f \| d_1 \| L_i S_i \rangle \sum_{m_i=1}^{3}\sum_{l_f=1}^{3} \left| \left[ \left(\mu_{m_i}+1/2\right)^2 - \left(l_f+1/2\right)^2 \right] \Im\left(\mu_{m_i}, k_{i'}, l_f, k_{f'}\right) \right|^2 \quad (2)$$

where

$$\Im\left(\mu_{m_i}, k_{i'}, l_f, k_{f'}\right) = \int_0^{\infty} \frac{1}{r} J_{\mu_{m_i}+1/2}(k_{i'} r)\, J_{l_f+1/2}\left(k_{f'} r\right) dr \quad (3)$$

can be calculated in terms of hypergeometric ${}_2F_1$ functions by many methods with good precision. $\varepsilon_{\min}$ is the lower cut-off in the integration over the energies of the perturber. The $J_\nu$'s are cylindrical Bessel functions. The lineshape can also be written:

$$I(\Delta\omega) = \sum_{L_i^T=0}^{L_D} I_{L_i^T}(\Delta\omega) = N_e \sum_{L_i^T=0}^{L_D} F_{L_i^T}(\Delta\omega) \quad (4)$$

where the cut-off $L_D$, corresponding to the Debye radius, takes into account the screening of the other electrons. The contribution of the first three angular momenta, $L_i^T = 0$, 1 and 2, which was shown to be the major contribution in the far wings, cannot be provided by the exact resonance method since in these cases, $\mu_{m_i}$ is not real. This contribution will be estimated in the present work by an extrapolation method (Sect. 4). $I_{L_i^T}(\Delta\omega)$ can also be decomposed into multipole contributions $I^{(\lambda)}_{L_i^T}(\Delta\omega)$, with $\lambda$=1, 2, and 3 for the dipole, quadrupole and polarization potentials (Tran Minh et al. 1980); but when these higher multipoles contribute significantly to the $e^-$–H potential, correlations between the atomic electron and the perturber become important and it is not sufficient to use a multipolar expansion for the potential. In particular, exchange effects become important.

## 3. Density effects

The aim of this section is to examine the density dependence of the lineshape. According to equation (4), this dependence is contained in the maximum angular momentum $L_D$, since $L_D \sim k\rho_D$, with $\rho_D$ Debye distance. Let us decompose the profile $I(\Delta\omega)$ of equation (4) into two terms denoted $I_1(\Delta\omega)$ and $I_2(\Delta\omega)$ so that:

$$I(\Delta\omega) = N_e \sum_{L_i^T=0}^{2} F_{L_i^T}(\Delta\omega) \quad (5)$$

$$I(\Delta\omega) = N_e \sum_{L_i^T=3}^{L_D} F_{L_i^T}(\Delta\omega) \quad (6)$$

and let us put

$$R_i(\Delta\omega) = I_i(\Delta\omega)/I_H(\Delta\omega) \quad (7)$$

where $I_H$ is the asymptotic Holtsmark profile, i.e:

$$I_H(\Delta\omega) = \pi\sqrt{3}\left(\frac{\hbar}{m}\right)^2 N_e |\Delta\omega|^{-5/2} \quad (8)$$

$R_1(\Delta\omega)$, which is the object of the next paragraph, is independent of the density. Hence, the density dependence comes from $R_2(\Delta\omega)$ via the limit $L_D$. We have calculated the latter contribution at various densities and temperatures.The results are reported in the Tables 1 to 3. It comes out from these tables that the influence of the density increases with the temperature, and that the density effect is meaningful only in the linecore and the near linewings ($|\Delta\lambda| < 8$ Å). For $|\Delta\lambda|$ greater than 8Å, the profile is linear in density, within an error less than 1%, at densities below $10^{17}\mathrm{cm}^{-3}$. This result is accounted for by the convergence of sum (6) at a value of $L_i^T$ lower than $L_D$.

At higher densities, gets smaller and the region of non-linearity enlarges. However, not too far in the line wings (detunings $|\Delta\lambda| < 80$ Å), $L_D$ is a good cut-off.

## 4. Extrapolation method for the contribution of the first three angular momenta to the total profile

Feautrier et al. (1976) and Feautrier and Tran Minh (1977) used two methods to determine the contribution of the first angular momenta ($L_i^T = 0$, 1 and 2), excluded by the exact resonance approximation. The first, based on the program of Seaton and Wilson (1972), consisted of solving the coupled integro-differential equation; and the second leaned on a semi-empirical approach. A rapid and accurate method is still needed for the calculation of this contribution. The present extrapolation procedure consists of continuing the curve of the contribution of the angular momenta to the total profile ($I_{L_i^T}(\Delta\omega) = f\left(L_i^T\right)$ ) such as to find the contributions relative to $L_i^T = 0$, 1 and 2 with the minimum error. A good choice for this extrapolation is obtained by completing the original curve by a straight line connecting the point $B(L_i^T = 3, I_3)$ to the point $A(L_i^T = 0, I_3/2)$ (Fig.1). The

**Table 1.** Values of $R_2(\Delta\omega)$ at $T$ = 2500K and various densities $N_e$ (in cm$^{-3}$). Each dash is to be read as the closest number on the right hand side of the same line. $E-m$ stands for $10^{-m}$.

| $\Delta\lambda$ (Å) | $N_e = 10^{14}$ | $N_e = 10^{16}$ |
|---|---|---|
| -90 | - | .9673E-2 |
| -60 | - | .4153E-1 |
| -40 | - | .1151 |
| -20 | - | .340 |
| -10 | - | .606 |
| -8 | - | .681 |
| -4 | - | .849 |
| -2 | .909 | .908 |
| 2 | .851 | .850 |
| 4 | - | .800 |
| 8 | - | .677 |
| 10 | - | .624 |
| 20 | - | .445 |
| 40 | - | .278 |
| 60 | - | .198 |
| 90 | - | .135 |

**Table 2.** Same as table 1 with $T$ = 10000K

| $\Delta\lambda$ (Å) | $N_e = 10^{14}$ | $N_e = 10^{16}$ |
|---|---|---|
| -90 | - | .2955 |
| -60 | - | .4523 |
| -40 | - | .606 |
| -20 | - | .807 |
| -10 | - | .606 |
| -8 | - | .901 |
| -4 | - | .880 |
| -2 | .795 | .791 |
| 2 | .770 | .765 |
| 4 | - | .835 |
| 8 | - | .851 |
| 10 | - | .843 |
| 20 | - | .768 |
| 40 | - | .622 |
| 60 | - | .519 |
| 90 | - | .414 |

contribution of the first three angular momenta is thus found to be:

$$\sum_{L_i^T=0}^{2} I_{L_i^T}(\Delta\omega) \approx 2I_3(\Delta\omega) \tag{9}$$

while the sum of errors due to extrapolation of the three points is about $I_3(\Delta\omega)$. On the other hand, since there is a balancing of the $I_{L_i^T}$'s in the sum around the extrapolation line, the actual error is about $I_3(\Delta\omega)/2$. Hence, the total profile, normalized

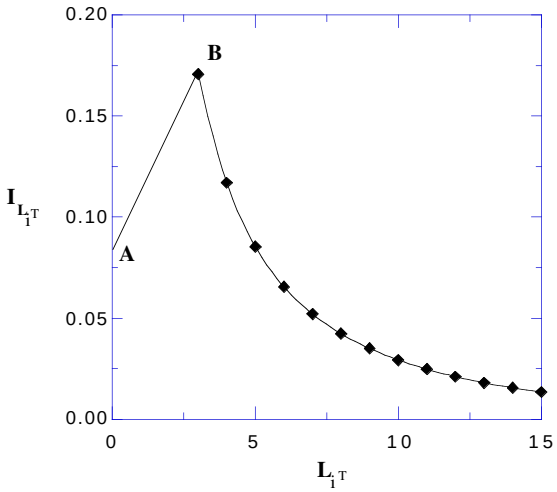


**Fig. 1.** Extrapolation of the contribution of the first three angular momenta to the total profile for $\Delta\lambda = -20$Å. Data from the exact quantum calculations are presented in Feautrier et al. (1976)

**Table 3.** Same as Table 1 with $T$ = 40000K

| $\Delta\lambda$ (Å) | $N_e = 10^{14}$ | $N_e = 10^{16}$ |
|---|---|---|
| -90 | - | .780 |
| -60 | - | .859 |
| -40 | - | .900 |
| -20 | - | .897 |
| -10 | - | .827 |
| -8 | - | .795 |
| -4 | .686 | .683 |
| -2 | .572 | .561 |
| 2 | .565 | .555 |
| 4 | .673 | .670 |
| 8 | - | .769 |
| 10 | - | .775 |
| 20 | - | .847 |
| 40 | - | .843 |
| 60 | - | .808 |
| 90 | - | .747 |

to $I_H(\Delta\omega)$ in the dipole approximation and taking into account each of the $L_i^T$'s contribution is:

$$I(\Delta\omega) = \frac{1}{I_H(\Delta\omega)}\left(2I_3(\Delta\omega) \pm \frac{1}{2}I_3(\Delta\omega)\right) + R_2(\Delta\omega) \tag{10}$$

Numerically, the error in the so-determined total profile is found to vary from about less than 5% in the near line wings to about less than 15% the far wings. Further, it decreases with increasing temperature. The present extrapolation procedure, which has been checked to provide results in good agreement with the semi-empirical method of Feautrier and Tran Minh (1977) is advantageous for its rapidity and its simplicity.

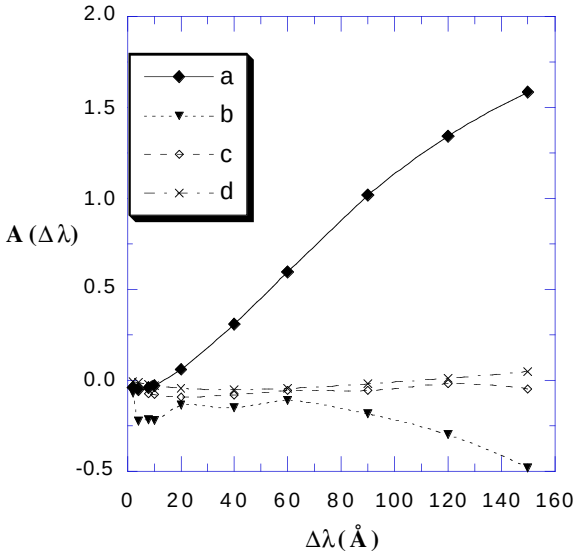


**Fig. 2.** Asymmetry of the total electronic profile; a corresponds to T=5000K, b to T=5000K(*), c to T=10000K(*) and d to T=40000K. The asterisks point out the cases where the short range effects (quadrupole + polarization) are taken into account.

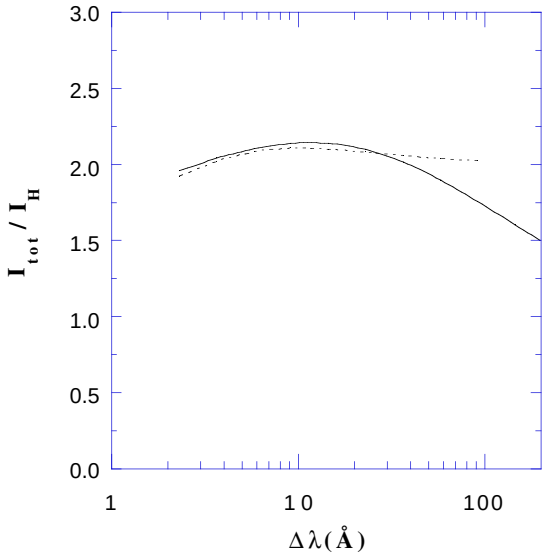


**Fig. 3.** Comparison of our results (full line) with those of Vidal et al. (VCS : dotted line) at $N_e = 10^{16}\mathrm{cm}^{-3}$ and $T = 10000$K. The total Holtsmark-normalized profile is plotted versus the detunings $\Delta\lambda$ (in Å).

## 5. Asymmetry

In electron broadening, asymmetry is due: firstly to the difference between the lower cut-offs ($\varepsilon_{\min}$) in the integration over the perturber energies for both wings; and secondly to the introduction of the short range potentials contribution. Therefore, in the dipole approximation, the asymmetry is expected to decrease as the temperature increases. The asymmetry of the profile is represented by the quantity:

$$A(\Delta\lambda) = 2\left(\frac{I(\Delta\lambda) - I(-\Delta\lambda)}{I(\Delta\lambda) + I(-\Delta\lambda)}\right) \tag{11}$$

The variations of $A(\Delta\lambda)$ due to the lower cut-off are presented in Fig. 2 at $T = 5000$ and 40000K. For comparison, short range effects due to quadrupole and polarization potentials (Tran Minh et al. 1980) are shown in Fig. 2 for $T = 5000$ and 10000K.

Fig. 2 leads to two main observations. At $T = 40000$K the asymmetry is very small (close to 0). This was to be expected since in this case the lower cut-off tends to $\varepsilon_{\min} = \hbar\omega/kT$ tends to 0. More generally, the asymmetry decreases with increasing temperature.

It is to be mentioned (Allard et al. 1994) that quasi-molecular effects due to $H - H^+$ and $H - H$ collisions are a source of asymmetry in the far wings. Further, when ions are included, they contribute significantly to asymmetry. These last two points have not been taken into account in our work since we are interested in the electronic contribution to the lineshapes.

## 6. Results and discussion

This section is concerned with the comparison of our calculations with the data of VCS on one hand, and the presentation of our results and their parametrization at various temperatures on the other hand. The data of VCS were compiled with a formalism based on the unified classical-path theory for electrons and the quasistatic approximation for ions (Vidal et al. 1971). These data have been the most reliable in the far wings for a long time although the electron description is not sufficient in the far wings.

### *6.1. Comparison with the data of Vidal et al.*

In Figs. 3 to 6, line profiles normalized to the asymptotic Holtsmark profiles, provided by both VCS and our formalism are reported. The ionic contribution is assumed to be quasistatic and thus is represented by unity. The Holtsmark-normalized profile is $1 + R(\Delta\omega) = 1 + R_1(\Delta\omega) + R_2(\Delta\omega)$. There is no need here to include the short range effects in our calculations since they are not taken into account by VCS.

One observes discrepancies in the far wings between our profiles and those of VCS. These discrepancies, which were already found between the semi-classical and the quantum theories (Tran Minh et al. 1975; Feautrier et al. 1976; Feautrier and Tran Minh 1977), imposed the use of quantum calculations in the far wings. At high temperatures - about 40000K - the discrepancies decrease, so that the quantum and semi-classical results are close; furthermore, our profiles are obtained with a better precision (10% in the far wings versus 15% at low temperatures). Stehlé (1994) used a semi-classical description for electrons and ions, so that the profile exhibits the same static limit

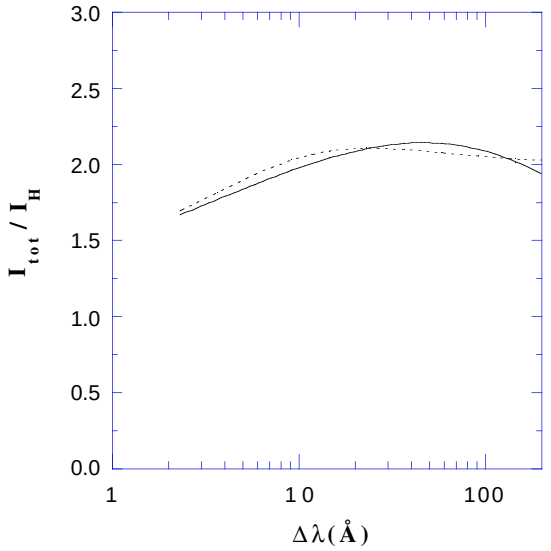


**Fig. 4.** Same as Fig. 3 for $N_e = 10^{15}\text{cm}^{-3}$ and $T = 40000$K.

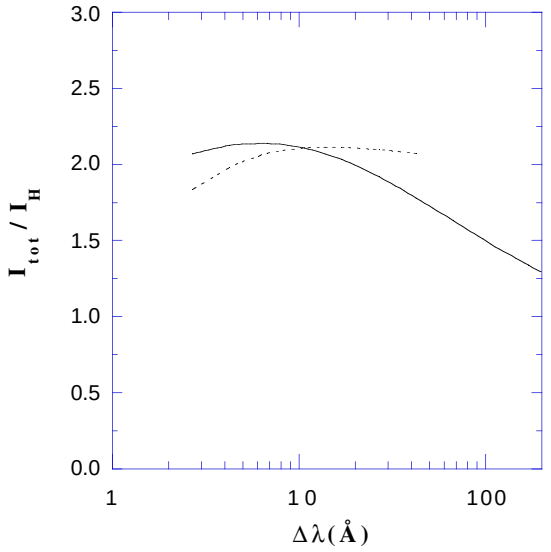


**Fig. 5.** Same as Fig. 3 for $N_e = 10^{17}\text{cm}^{-3}$ and $T = 5000$K.

as VCS in the line wings, leading to the well known $|\Delta\omega|^{-5/2}$ variation of the intensity. In this case, the Holtsmark-normalized profile is taken to be 2 at large detunings $|\Delta\lambda|$.

It is important to mention that at large detunings, short range effects contribute significantly to the profile and have to be taken into account. Nevertheless, not too far in the wings the dipole approximation holds. Hence our calculations are carried out for detunings not exceeding 80Å.

### *6.2. Results and parametrized profiles at various temperatures*

The results are available upon request for electron densities $N_e$ varying from $10^{12}$ to $10^{16}\text{cm}^{-3}$, in the form presented in Table 4. They have been parametrized to facilitate their use. In fact, in the one perturber theory, the electronic line profile reads:

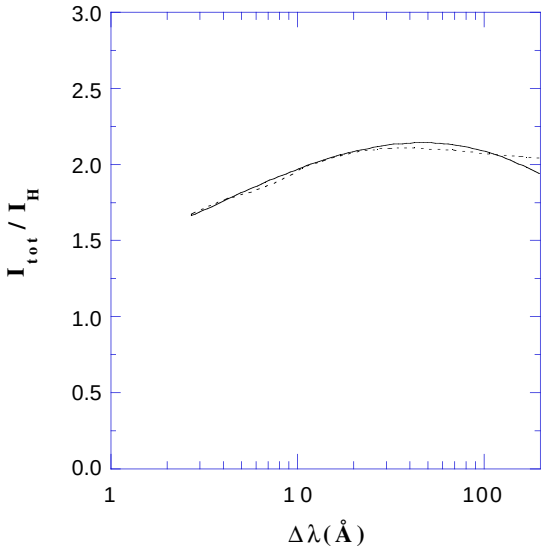


**Fig. 6.** Same as Fig. 3 for $N_e = 10^{17}\text{cm}^{-3}$ and $T = 40000$K.

$$I(\Delta\omega) = \frac{\gamma(\Delta\omega)}{2\pi\Delta\omega^2} \tag{12}$$

where the collisonal width $\gamma(\Delta\omega)$ can be expressed from equation (2). Without the $\Delta\omega$-dependence of $\gamma$, the Holtsmark-normalized profile would scale like $\Delta\omega^{-1/2}$. The decreasing of this profile at large detunings is due to a combination with other powers of $\Delta\omega$. In any case, the Holtsmark-normalized profile $R(\Delta\lambda)$ can be represented for both wings by a polynomial in $\Delta\lambda$ at any temperature within less than 5%.

Let us put $x = \Delta\lambda$ for the red wing and $x = -\Delta\lambda$ for the blue wing, and let us call $R_{red}(\Delta\lambda)$ the red wing Holtsmark-normalized profile and the $R_{blue}(\Delta\lambda)$ blue wing one. The Lyman-$\alpha$ profiles can be fitted for $2 \leq |\Delta\lambda| \leq 80$Å by polynomials, so that one has:

$$R_{red}(x) = \sum_{i=0}^{n} a_i x^i \tag{13}$$

and

$$R_{blue}(x) = \sum_{i=0}^{n} b_i x^i \tag{14}$$

The coefficients $a_i$ and $b_i$ are reported in Tables 5 to 8 for $T =$ 2500, 5000, 10000, 20000 and 40000K and the density $N_e = 10^{15}\text{cm}^{-3}$. In some cases, the profiles are not fitted completely by only one polynomial. A suitable value of $x$ is found such as to fit the profiles by two different polynomials corresponding to the ranges of $x$ below and above this value.

At high temperatures the coefficients corresponding to the same order of get closer as $T$ increases. This is to be accounted for by the decreasing asymmetry of both wings with increasing temperature.

**Table 4.** Holtsmark-normalized wings profile of Hydrogen Lyman-$\alpha$ line at $N_e$ = $10^{15}$cm$^{-3}$ and $T$ = 40000K. The error is that made in the contribution of the first angula momenta to the total profile by the extrapolation method.

| $\Delta\lambda$ (Å) | $R(\Delta\lambda)$ | Error (%) |
|---|---|---|
| -200 | 0.834 | 9.32 |
| -150 | 0.963 | 8.68 |
| -120 | 1.044 | 8.21 |
| -90 | 1.124 | 7.65 |
| -60 | 1.188 | 6.92 |
| -40 | 1.200 | 6.24 |
| -20 | 1.134 | 5.23 |
| -10 | 1.005 | 4.43 |
| -8 | 0.957 | 4.21 |
| -4 | 0.803 | 3.65 |
| -2 | 0.655 | 3.23 |
| 2 | 0.651 | 3.32 |
| 4 | 0.793 | 3.80 |
| 8 | 0.935 | 4.43 |
| 10 | 0.977 | 4.67 |
| 20 | 1.087 | 5.52 |
| 40 | 1.142 | 6.55 |
| 60 | 1.139 | 7.25 |
| 90 | 1.103 | 8.05 |
| 120 | 1.058 | 8.67 |
| 150 | 1.011 | 9.19 |
| 200 | 0.939 | 9.89 |

**Table 5.** Coefficients $a_i$ and $b_i$ for $T$ = 2500K and 5000K.

| | $T$ = 2500K | | $T$ = 5000K | |
|---|---|---|---|---|
| $i$ | $a_i$ | $a_i$ | $b_i$ | $b_i$ |
| 0 | 1.209 | 1.332 | 1.168 | 1.2703 |
| 1 | -2.474E-2 | -4.756E-2 | -1.041E-2 | -2.0782E-2 |
| 2 | 2.861E-2 | 6.540E-4 | 4.437E-5 | 1.1643E-4 |
| 3 | -1.776E-6 | -4.213E-6 | -7.012E-8 | -2.1906E-7 |
| 4 | 5.363E-9 | 1.241E-8 | 0. | 0. |
| 5 | -6.042E-12 | -1.293E-11 | 0. | 0. |

**Table 6.** Coefficients $a_i$ and $b_i$ for $T$ = 10000K.

| $i$ | $a_i$ | $b_i$ |
|---|---|---|
| 0 | .8599 | .8625 |
| 1 | 5.5459E-2 | 6.7732E-2 |
| 2 | -3.5113E-3 | -4.3723E-3 |
| 3 | 9.4223E-5 | 1.1553E-4 |
| 4 | -1.3255E-6 | -1.6083E-6 |
| 5 | 1.0061E-8 | 1.2132E-8 |
| 6 | -3.8799E-11 | -4.6605E-11 |
| 7 | 5.9351E-14 | 7.111E-14 |

**Table 7.** Coefficients $a_i$ and $b_i$ for $T$ = 20000K.

| $i$ | $a_i(x\leq 60)$ | $a_i(x\geq 60)$ | $b_i(x\leq 60)$ | $b_i(x\geq 60)$ |
|---|---|---|---|---|
| 0 | .64303 | 1.2687 | .63871 | 1.4244 |
| 1 | 9.2019E-2 | -3.8789E-3 | 9.9951E-2 | -6.97E-3 |
| 2 | -6.6988E-3 | 5.8917E-6 | -7.034E-4 | 1.1643E-4 |
| 3 | 2.4864E-4 | 0. | 2.5443E-4 | 0. |
| 4 | -5.1838E-6 | 0. | -5.2382E-6 | 0. |
| 5 | 6.2257E-8 | 0. | 6.2496E-8 | 0. |
| 6 | -4.2454E-10 | 0. | -4.2454E-10 | 0. |
| 7 | 1.5182E-12 | 0. | 1.5147E-12 | 0. |
| 8 | -2.1994E-15 | 0. | -2.1909E-15 | 0. |

**Table 8.** Coefficients $a_i$ and $b_i$ for $T$ = 40000K.

| $i$ | $a_i$ | $b_i$ |
|---|---|---|
| 0 | .5387 | .5362 |
| 1 | 7.1498E-2 | 7.4966E-2 |
| 2 | -3.515E-3 | -3.5629E-3 |
| 3 | 8.8432E-5 | 8.807E-5 |
| 4 | -1.2143E-6 | -1.2E-6 |
| 5 | 9.1095E-9 | 8.9783E-9 |
| 6 | -3.4899E-11 | -3.434E-11 |
| 7 | 5.3167E-14 | 5.2266E-14 |

## 7. Conclusion

In the dipole approximation, the quantum unified theory shows a linear dependence of the electronic line profile of the Hydrogen Lyman-$\alpha$ line on the density for detunings above 8Å or below $-8$Å. Between these two limits, the density dependence of the profile is more complex. Further, this profile is strongly influenced by the temperature at low temperatures. At high temperatures, the asymmetry of the profile vanishes; and our results are in good agreement with those of VCS. The extrapolation method used here allows us to calculate the profile in the far wings of Lyman-$\alpha$ within an acceptable precision (from 15% at 2500K to less than 9% at 40000K). The polynomial fit of our results permits their easy reproduction.

Our calculations are restricted to detunings $|\Delta\lambda|$ not exceeding 80Å so that the contribution of short range effects on the profile is less important.The cut-off procedure on the angular momenta is good for these detunings. Next, we shall study from a quantum point of view the contribution of these short range interactions, as well as the ion contribution to the far wings.

*Acknowledgements.* The author would like to acknowledge Dr. Nicole Feautrier for suggesting this work, and Dr. N. Tran Minh for fruitful discussions.

## References

Allard N., Koester D., Feautrier N. and Spielfiedel A. 1994, A&A 200, 58

Boldt G. and Cooper W. S. 1964, Z. Naturf. 19a, 968

Caby-Eyraud M., Coulaud G. and Nguyen Hoe 1975, J.Q.S.R.T. 15, 593
Feautrier N. and Tran Minh N. 1977, J. Phys. B: Atom. Molec. Phys. 10, 3427
Feautrier N., Tran Minh N. and Van Regemorter H. 1976, J. Phys. B: Atom. Molec. Phys. 9, 1871
Fussmann G. 1975, J. Quant. Spectroc. Radiat. Transfer. 15, 819
Günter S. and Könies A. 1994, J. Quant. Spectroc. Radiat. Transfer. 52, 819
Könies A. and Günter S. 1994, J. Quant. Spectroc. Radiat. Transfer. 52, 825
Lisitsa V. S. and Sholin G.V. 1972, Sov. Phys.-JETP 34, 484
Tran Minh N, Feautrier N and Van Regemorter H 1975, J. Phys. B: Atom. Molec. Phys 8, 1810
Tran Minh N. and Van Regemorter H. 1972, J. Phys. B: Atom. Molec. Phys. 5, 903
Tran Minh N, Feautrier N and Edmonds A. R. 1980, J.Q.S.R.T 23, 377
Seaton M. J. and Wilson P. M. H. 1972, J. Phys. B: Atom. Molec. Phys. 5, L1
Stehlé C. 1994, A&AS. 104, 509
Van Regemorter H. 1969, Phys. Lett. 30A, 365
Vidal C. R., Cooper J. and Smith E. W. 1971, Nat. Bur. Stand. (U.S.), Monograph 120
Vidal C. R., Cooper J. and Smith E. W. 1973, ApJS, 25, 37
Voslamber D. 1972, Z. Naturf. 27a, 1789

This article was processed by the author using Springer-Verlag LaTeX A&A style file *L-AA* version 3.